Analysis of potentialities of using radiative excitation of water vapor molecules to control thermodynamics of phase transitions

V.I. Starikov and Yu.D. Kopytin

Institute of Atmospheric Optics,
Siberian Branch of the Russian Academy of Sciences, Tomsk

Received April 20, 2000

The efficiency of the nonlinear mechanism of changing the H_2O intermolecular interaction potential due to radiative excitation of rotational-vibrational transitions is studied. It is shown that the corresponding short-term changes of the virial coefficients in the equation of state of a nonideal gas can provide for transition of the atmospheric seed nuclei through the forbidden size zone to the zone of condensation-active droplets thus initiating the high-energy macroprocess of removing excess supersaturation in a medium at phase transition.

Introduction

The search for new mechanisms to control atmospheric macroprocesses, including formation of precipitation, by high-power electromagnetic impact is an urgent task. Such a control becomes possible thanks to advances in related fields of fundamental science and development of technologies for the creation and use of high-power lasers and other sources of electromagnetic radiation, physics of low-temperature plasma and thermodynamics of phase transitions.[1–4]

When studying the interaction of high-intensity laser radiation with a matter, the possibility of stimulating by radiation the phase transitions in the matter is very interesting. In contrast to well-known photochemical mechanisms of generation of the seed condensation nuclei, the coexistence curve of two phases can change its position, in particular, due to nonlinearity of the Van-der-Waals interaction of molecules or atoms at their radiative excitation. The mechanism of this nonlinearity was discussed in Refs. 5–7.

In this paper, we consider the efficiency of electromagnetic mechanisms of initiating phase transitions by simulating the processes changing the H_2O intermolecular interaction potential due to radiative excitation of the corresponding rotational-vibrational transitions.

1. Initial set of nonlinear equations and relations for simulating phase transitions under electromagnetic impact

It is known that the processes of formation of the liquid-droplet phase in the atmosphere mostly occur due to condensation on seed particles of admixtures (water solutions of salts). The minimum size of seeds depends on the pressure of saturated vapor in a medium and on the physical and chemical properties of the particulate matter. The corresponding basic nonlinear equations of the process with the allowance made for radiative excitation of water vapor molecules have the following form:

$$dr/dt = D(\rho_v/\rho_l)\,(\delta/r); \qquad (1)$$

$$(1-\delta)/(1-\delta_0) = 1 + bx - cx^3; \qquad (2)$$

$$\delta = (p_\infty/p_r - 1),\ \delta_0 = (p_\infty/p_0 - 1),\ x = 1/r; \qquad (3)$$

$$V\,p_0/RT = 1 + B(T)/V + C(T)/V^2 + \ldots, \qquad (4)$$

$$B(T) = b_0 B^*(T^*, t^*), \quad C(T) = b_0^2 C^*(T^*, t^*),$$
$$T^* = kT/\varepsilon,\ t^* = 8^{-1/2}\,\mu^2/\varepsilon\sigma^3, \qquad (5)$$

$$V^{Sc} = (4\varepsilon[(\sigma/r)^{12} - (\sigma/r)^6] -$$
$$- (2\cos\theta_a\cos\theta_b - \sin\theta_a\sin\theta_b\cos(\varphi_a - \varphi_b))\mu_a\mu_b/r^3, \qquad (6)$$

$$\tilde{\mu}_z^v(n) = \sum_\alpha \Phi_\alpha\ {}^v\tilde{\mu}_\alpha^e(n) + \frac{1}{2}\sum_{\alpha,\beta,\gamma}\{\Phi_\alpha, J_\beta J_\gamma\}^{\alpha,\beta\gamma}\tilde{M}_2(n); \qquad (7)$$

$$\eta(n, J) = \left(\frac{\mu(n, J)}{\mu(n=0, J=0)}\right)^4 > 1. \qquad (8)$$

Here Eq. (1) is the equation of condensation growth of droplets; Eq. (2) is the equation for δ_r – supersaturation near the surface of a condensation nucleus of the radius r; $p_0(T, I)$ and $p_r(T, I)$ are the saturated vapor pressure over the plane water surface and near the nucleus surface, respectively; they functionally (nonlinearly) depend on the intensity of incident radiation (for example, laser radiation); $b = 2\sigma_s\,(R_v T\rho_v)^{-1}$; $c = A_1\,m$; σ_s and ρ_v are the surface tension and density of the solution; m is the nucleus mass; c is the activity of the condensation nucleus; r is the nucleus radius; R_v and T are the gas constant and temperature of the vapor; A_1 is the coefficient accounting for the pressure decrease due to molecules of the dissolved matter; p_∞ is the pressure of saturated vapor; Eq. (4) is the general form of the virial equation of the state of water vapor as of a nonideal gas; V, R,

0235-6880/00/05 437-06 $02.00

$B(T)$, and $C(T)$ are the volume, universal gas constant, and the second and third virial coefficients, respectively. One can use the two-parameter Van-der-Waals equations like:

$$(p_0 + a/V)(V - b) = RT; \quad B(T) = b - a/RT; \quad C(T) = b^2, \tag{9}$$

where a and b are the empirical parameters related to the virial coefficients $B(T)$ and $C(T)$; Eq. (6) is the model Schtokmaier potential[8] describing the intermolecular interaction; ε and σ are the parameters of the Lenard–Johns potential; μ_a and μ_b are the dipole moments of the molecules a and b. The values $\eta > 1$ in Eq. (8) are indicative of an increase in the dipole-dipole attraction forces at rotational-bending excitation of the corresponding transitions in water vapor molecules, while the values $\eta < 1$ are indicative of their decrease.

Thus, according to Eqs. (1)–(9), to study the influence of rotational-vibrational excitation on the equation of state of water vapor and heterogeneous condensation, one should analyze, first of all, the dependence of the molecular dipole moment on vibrational and rotational quantum numbers.

2. Calculation of nonlinearity of dipole moment and intermolecular potential for excited states of H_2O molecule

The H_2O molecule is classified, in the molecular rotational-vibrational spectroscopy, as a nonrigid molecule, since it exhibits a large-amplitude bending vibration. This bending or deformation vibration is associated with the change of the angle ∠HOH (for details see Ref. 8).

The properties of the water vapor molecule under study[7] are, first, the behavior of the effective dipole moment of the molecule in different rotational-bending states $(n, J) = (n \equiv v_2,\ J, K_a, K_c)$ (J, K_a, and K_c are the rotational quantum numbers) and, second, the influence of changes in the dipole moment in these states on some thermophysical characteristics of water vapor.

Variations (at rotational-bending excitation) of the virial coefficients and the corresponding Van-der-Waals coefficients, as well as the Joule–Thomson coefficient and diffusion coefficient in the mixtures of water vapor with nonpolar gases are considered.

A. Effective dipole moment

Among various types of vibrational excitation, the excitation of bending mode and rotation of a molecule about the axis corresponding to its least moment of inertia cause the most significant changes in the molecular configuration.

The dependence of the H_2O dipole moment on the rotational-bending states was calculated based on the relations for the effective dipole moment operator of a nonrigid molecule of the H_2X type.[10] The effective dipole moment operator, in the case of rotational operators, has the form (7), accurate to the second power terms. Here Φ_α are the directional cosines relating the axis Z of the spatial coordinate system and the molecular system of axes, J_β and J_γ ($\alpha, \beta, \gamma = x, y, z$) are the components of the operator of the total angular momentum in the molecular system of axes, braces denote anticommutator, and the index v marks vibrational quantum numbers corresponding to a small-amplitude vibration. The molecular system of axes is taken the same as in Ref. 10. For the parameters ${}^{v}\tilde{\mu}^{e}_{\alpha}(n)$ and ${}^{\alpha,\beta\gamma}\tilde{M}_2(n)$ the following equations were derived in Ref. 10:

$$ {}^{v}\tilde{\mu}^{e}_{\alpha}(n) = \mu^{e}_{\alpha}(n) + \sum_{k\neq 2}\left(v_k + \frac{1}{2}\right)\times \times\left\{\frac{1}{2}\mu^{kk}_{\alpha}(n) - \frac{1}{2}\sum_i \frac{\mu^{i}_{\alpha}(n)\,\phi_{ikk}(n)}{\omega_i} - \sum_s \frac{\tilde{\phi}_{kk}(ns)\,\mu^{e}_{\alpha}(sn)}{\Omega_{sn}}\right\}, \tag{10}$$

$$ {}^{\alpha,\beta\gamma}\tilde{M}_2(n) = 2\sum_s \frac{B_\beta(ns)\,\mu^{e}_{\alpha}(sn)}{\Omega_{ns}}\,\delta_{\beta\gamma} - \sum_k \frac{B^{\beta\gamma}_{k}(n)\,\mu^{k}_{\alpha}(n)}{\omega_k} + + S^{(n)}_{111}\sum_\delta \varepsilon_{\beta\delta\gamma}\left(\delta_{\alpha\gamma}\,\mu^{e}_{\beta}(n) - \delta_{\alpha\beta}\,\mu^{e}_{\gamma}(n)\right). \tag{11}$$

In these equations

$$f(nm) = \langle \psi_n(\rho)\,|f(\rho)|\,\psi_m(\rho)\rangle,\ f(n) = f(nn); \quad \Omega_{nm} = E_n - E_m, \tag{12}$$

$f(\rho)$ are the functions of two types: the first type – functions $\phi(\rho)$ – is determined by the form of the rotational-vibrational Hamiltonian of a nonrigid molecule (it is chosen in accordance with Ref. 11), the second type – functions $\mu(\rho)$ – simulate the surface of the dipole moment of the molecule (ρ is the coordinate of the bending vibration from Ref. 11). Thus, to determine the coefficients ${}^{v}\tilde{\mu}^{e}_{\alpha}(n)$ and ${}^{\alpha,\beta\gamma}\tilde{M}_2(n)$ the following parameters should be known: (1) functions $f(\rho)$, (2) energies E_n and wave functions $\psi_n(\rho)$ associated with the large-amplitude bending vibration. The form of the functions $\phi(\rho)$ is given in Refs. 11–13; to calculate $\phi(\rho)$ needed in simulating the intramolecular potential function we used the force parameters from Ref. 13. The energies E_n and wave functions $\psi_n(\rho)$ were found by numerical integration of the corresponding Schrödinger equation[11] by the Numerov–Cooley method,[14] in which the function $V_0(\rho)$ determining the cross section of the molecular potential along the coordinate ρ was taken in the form

$$V_0(\rho) = f_{\alpha\alpha}\,\rho^2 + h(1 + f_{\alpha\alpha}\,\rho_e^2/h)^2/(1 + h\rho^2/f_{\alpha\alpha}\,\rho_e^4), \tag{13}$$

in which $f_{\alpha\alpha} = 12857.902$ cm^{-1}, $h = 10960.76$ cm^{-1}, and $\rho_e = 1.82083$ rad. The parameter h determines the

barrier for the linear configuration of the molecule. Numerical integration of the Schrödinger equation yields the following values of the frequencies $\Omega_{n0} = E_n - E_0$ (in cm^{-1}):

Frequency	Calculated	Experimental
Ω_{10}	1593.4	1594.8
Ω_{20}	3151.4	3151.5
Ω_{30}	4666.3	4666.6
Ω_{40}	6142.0	6134.3

The parameter $S_{111}^{(n)}$ for each n was calculated by the equation from Ref. 15. Finally, the functions $\mu_\alpha^e(\rho)$, $\mu_\alpha^1(\rho)$, and $\mu_z^3(\rho)$ from the series expansion

$$\mu_\alpha(\rho, q) = \mu_\alpha^e(\rho) + \sum_i \mu_\alpha^i(\rho)\, q_i + \frac{1}{2}\sum_{i,j} \mu_\alpha^{ij}(\rho)\, q_i\, q_j + \ldots \quad (14)$$

of the molecular components μ_α of the dipole moment over the dimensionless coordinates q_i describing the small-amplitude vibrations were chosen in the following form:

$$\mu_x^\sigma(\rho) = a_1 \sin(\rho/2) + a_2 \sin^2(\rho/2) + a_3 \sin^3(\rho/2), \quad (15)$$

$$\mu_z^3(\rho) = b_1 \cos(\rho/2) + b_2 \cos^2(\rho/2) + b_3 \cos^3(\rho/2) \quad (16)$$

(here σ is e or 1). The parameters a_i and b_i (i = 1, 2, 3) can be found in Ref. 10.

For the parameters $\mu_{xx}^{kk}(n)$ the following values were used: $\mu_{xx}^{11}(n) = 9 \cdot 10^{-3}$ D, $\mu_{xx}^{33} = -7 \cdot 10^{-3}$ D (for all n). Table 1 gives the calculated coefficients ${}^v\tilde{\mu}_\alpha^e(n)$ and $\tilde{M}_2(n)$ at n = 0, 1, ..., 4.

Table 1. Calculated parameters ${}^v\tilde{\mu}_\alpha^e(n)$ and ${}^{\alpha,\beta\gamma}\tilde{M}_2(n)$ for H_2O molecule (in D)

Parameter	n = 0	n = 1	n = 2	n = 3	n = 4
${}^{v=0}\tilde{\mu}_\alpha^e(n)$	−1.8543	−1.8255	−1.7907	−1.7475	−1.6910
${}^{x,xx}\tilde{M}_2(n)$	$2.6 \cdot 10^{-4}$	$3.0 \cdot 10^{-4}$	$3.6 \cdot 10^{-4}$	$4.3 \cdot 10^{-4}$	$5.3 \cdot 10^{-4}$
${}^{x,yy}\tilde{M}_2(n)$	$0.4 \cdot 10^{-5}$	$0.5 \cdot 10^{-5}$	$0.6 \cdot 10^{-5}$	$0.8 \cdot 10^{-5}$	$0.1 \cdot 10^{-4}$
${}^{x,zz}\tilde{M}_2(n)$	$-0.9 \cdot 10^{-3}$	$-1.5 \cdot 10^{-3}$	$-2.4 \cdot 10^{-3}$	$-4.4 \cdot 10^{-3}$	$-10 \cdot 10^{-3}$
${}^{y,xy}\tilde{M}_2(n)$	$-1.7 \cdot 10^{-4}$	$-2.0 \cdot 10^{-4}$	$-2.3 \cdot 10^{-4}$	$-2.6 \cdot 10^{-4}$	$-3.1 \cdot 10^{-4}$
${}^{z,xz}\tilde{M}_2(n)$	$2.4 \cdot 10^{-4}$	$2.6 \cdot 10^{-4}$	$2.9 \cdot 10^{-4}$	$3.2 \cdot 10^{-4}$	$3.7 \cdot 10^{-4}$

In our calculations, we used the factor 0.9916 for the coefficients a_i and b_i from Eqs. (15), (16), and equations given in Ref. 10, to achieve the closest agreement with the experimental data on the dipole moment obtained at low values of the rotational-bending quantum numbers.

B. Effective dipole moment in a rotational-bending state

The parameters ${}^v\tilde{\mu}_\alpha^e(n)$ and ${}^{\alpha,\beta\gamma}\tilde{M}_2(n)$ given in Table 1 allow calculating the mean values of the dipole moment as a matrix element

$$\mu(n, J) = \mu(n, J, K_a, K_c) =$$

$$= \langle \psi_{\text{rot}}^{(n)}(J, K_a, K_c) \,|\tilde{\mu}_x(n)|\, \psi_{\text{rot}}^{(n)}(J, K_a, K_c) \rangle \quad (17)$$

of the molecule-fixed x-component of the effective dipole moment. It follows from the symmetry properties of the H_2O molecule that only $\langle \psi_{\text{rot}}^{(n)}(J, K_a, K_c) \,|\tilde{\mu}_x(n)|\, \psi_{\text{rot}}^{(n)}(J, K_a, K_c) \rangle$ is nonzero.

The coefficients $C_k^{(n)}$ from the series expansion of the rotational wave function $|\psi_{\text{rot}}^{(n)}(J, K_a, K_c)\rangle = \sum_k C_k^{(n)} |J, K, \Gamma\rangle$ were calculated by reducing the matrix of the effective rotational Hamiltonian $H^{(n)}$ to the diagonal form for a series of bending vibrational states ($0\ n = v_2\ 0$) with n = 0, ... , 4 ($|J, K, \Gamma\rangle$ are the rotational symmetrized functions of a rigid top; Γ indicates the symmetry type). The form of the rotational Hamiltonian $H^{(n)}$ is given in Ref. 16; the Hamiltonian parameters were determined from the least-square fit to experimental energy levels of the water vapor molecule. The values of the dipole moment $\mu(n, J)$ were determined for $n \le 4$ and $J \le 14$.

Table 2 compares the calculated values of $\mu(n, J)$ at n = 0 and $J \le 2$ with the experimental values μ_{Shostak} found in Stark measurements and with μ_{MORBID} calculated by Mengel and Ensen (the values μ_{Shostak} and μ_{MORBID} were taken from Ref. 17). The results are in close agreement and confirm the correctness of the selected model of the dipole moment surface.

Table 2. Calculated and experimental values of dipole moment of H_2O molecule, in D

$(v_1\ n \equiv v_2\ v_3)$	$J\ K_a\ K_c$	μ_{Shostak}	μ_{MORBID}	This paper
(000)	111	1.855300	1.85538	1.8553
	110	1.855483	1.85513	1.8550
	211	1.852519	1.85446	1.8543
(010)	110	1.82401	1.82432	1.8252
	111	1.82361	1.82405	1.8266
	211	1.82061	1.82330	1.8258

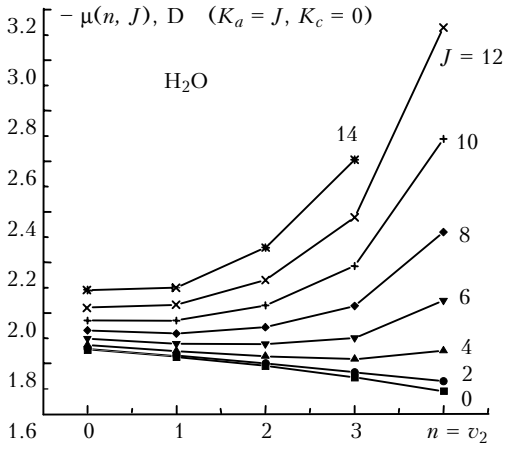

Fig. 1. The dipole moment of H_2O molecule in different rotational-vibrational states.

Because the calculated results are too cumbersome, they are presented graphically (Figs. 1 and 2). Figure 1 shows the dipole moment of the molecule in the rotational states $[J, K_a = J, K_c = 0]$ as a function of the bending quantum number $n \equiv v_2$.

The behavior of the dipole moment in different bending vibrational states is shown in Fig. 2 as a function of the rotational quantum number K_a (for $J = 10$).

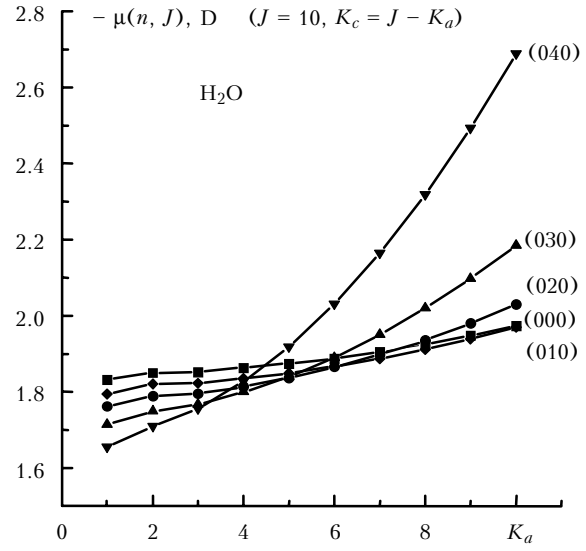

Fig. 2. The dipole moment of H_2O molecule vs. quantum number K_a ($J = 10$, $K_c = J - K_a$).

It follows from Fig. 2 that variations of the dipole moment of the water vapor molecule at rotational-bending excitation can be quite significant.

C. Intermolecular potential caused by the dipole-dipole interaction

The contribution to the intermolecular potential due to dipole-dipole interaction between the molecules a and b, upon averaging over spatial orientations, is determined by the following equation[18]:

$$V^{\mathrm{d.d}} = -\frac{2}{3kT}\frac{(\mu_n^a)^2\,(\mu_m^b)^2}{r^6}, \qquad (18)$$

where n and m are quantum numbers; k is the Boltzmann constant; T is temperature; r determines the separation between the molecules. It is convenient to introduce the parameter η given by Eq. (8) to characterize the influence of variations of the dipole moment on the value $V^{\mathrm{d.d}}$ for two water vapor molecules being in the same rotational-bending quantum state (n, J). The value $\eta > 1$ is indicative of an increase in the dipole-dipole forces.

It was found that $0.7 \le \eta \le 4.5$ for the quantum numbers $0 \le n \le 4$ and $0 \le J \le 10$, $\eta(n = 0, J) > 1$ for $K_a \ge 2$, $\eta(n = 1, J) > 1$ for $K_a \ge 3$, $\eta(n = 2, J) > 1$ for $K_a \ge 4$–5, $\eta(n = 3, J) > 1$ for $K_a \ge 5$, and $\eta(n = 4, J) > 1$ for $K_a \ge 5$.

3. Variations of thermodynamic characteristics of water vapor and condensation activity of Aitken nuclei with water vapor molecules being in excited states

The obtained values of the effective dipole moment in different rotational-bending states allowed variations of different thermodynamic characteristics of water vapor to be calculated. Below we consider, for simplicity, the limiting case of 100% excitation of water vapor molecules exposed to radiation without any regard of the specific mechanism and intensity of incident radiation. The problem of excitation of water vapor molecules calls for a separate study. Forbidden (metastable) transitions without radiative decay of the excited states are apparently most interesting from this point of view.

Using the potential V^{Sc}, the second virial coefficient $B(T)$ can be calculated as $B(T) = b_0 B^*(T^*, t^*)$. In this equation $T^* = kT/\varepsilon$; $t^* = 8^{-1/2}\,\mu^2/\varepsilon\sigma^3$, μ is the dipole moment of the molecule; b_0 is the constant factor equal to 23.43 cm^3/mol. The value $B^*(T^*, t^*)$ calculated at different temperature and different t^* has been tabulated in Ref. 9 (Table XVII), while Table XX in this same Ref. 9 gives the values of $C^*(T^*, t^*)$ that determine the third virial coefficient $C(T)$ according to the equation $C(T) = b_0^2 C^*(T^*, t^*)$.

The main contribution to such thermodynamic parameters as free energy, entropy, enthalpy, and Joule–Thomson coefficient is determined by the second virial coefficient and its temperature derivative. The Joule–Thomson coefficient μ^0 is determined as

$$B_1^*(T^*, t^*) - B^*(T^*, t^*) = \mu^0\, C_p^0/b_0,$$

where C_p^0 is the heat capacity reduced to the zero pressure $P = 0$. The values $B_1^*(T^*, t^*) - B^*(T^*, t^*)$ are given in Table XVIII in Ref. 9. The diffusion and viscosity coefficients of the mixture of polar and nonpolar gases can, by analogy, be considered among the transfer coefficients.

The curves like $\delta_0 = (p_\infty/p_r - 1)$, in accordance with Eq. (2), present the family of parabolas for condensation growth of nuclei with fixed δ_0 and activity c. Apparently, there exists (see, e.g., Ref. 5) a critical value of the nucleus activity $c_k = (4b^3/27)\{(1 - \delta_0)/\delta_0\}^2$, which corresponds to the parabola tangent to the axis. Nuclei with $c > c_k$ grow unlimitedly and transform into macrodrops. The intersection of the parabola with the abscissa ($\delta = 0$) at

$c < c_k$ at two points determines the zone of forbidden size of nuclei:

$$\Delta r = (3c/4b)^{1/2}[\cos^{-1}(\pi/3 + \arccos(c/c_k)^{1/2}/3) - \cos^{-1}(\pi/3 - \arccos(c/c_k)^{1/2}/3)]. \quad (19)$$

At a pulsed action of, for example, resonance transition of laser radiation, extra effective supersaturation $(\delta_0 + \delta_N)$ arises because of the nonlinear change of the dipole moment of the water vapor molecule with $\eta > 1$. In this case, the concentration of nuclei with $c > c_k$ increases for a while, and the nuclei start to grow due to condensation. Microdroplets (nuclei), which succeed to overcome the zone of forbidden size Δr for the lifetime of resonance excitation t_{res}, grow unlimitedly and transform into macrodrops.

Thus, in Refs. 5 and 6 the equations were derived, for example, for the Junge size-distribution of nuclei $n(r_0) = n_1 r_0^{-z}$ where n_1 and z are parameters, and for the time of transition of the Aitken nuclei through the zone of forbidden size as a function of the nonlinear parameter $(\delta_0 + \delta_N)$.

The estimates showed that avalanche macroprocesses of removing the excess supersaturation can occur in the considered cases because of the mechanisms of radiative excitation of water vapor molecules, nucleus charging, and intensification of coagulation of thus formed aerosol droplets. By energy, these processes significantly, by 10^6–10^7 times, exceed the initial electromagnetic energy deposited to the medium.

Below, we present, for illustration, the results obtained by simulating various thermodynamic characteristics of water vapor based on calculations of the effective dipole moment in different rotational-bending states.

Figure 3 shows the variations of $B^*(T^*, t^*)$ at $T = 380$ K. This parameter determines, via the Eq. (5), the second virial coefficient and, correspondingly, the Van-der-Waals parameters. For the Lenard–Johns intermolecular potential, we used the parameters $\varepsilon/k = 380$ K and $\sigma = 2.65\ \Delta$ found from the experimental value of the second virial coefficient $B(T)$ of the H_2O molecule[17] at $t^* = 1.2$ ($\mu = -1.834$ D); in this case $b_0 = 23.43\ cm^3/mol$. Note that the virial coefficients and the Van-der-Waals coefficients can vary widely. Figure 4 shows the variations of $B_1^*(T^*, t^*) - B(T^*, t^*)$ at $T = 100°C$ (this difference determines the Joule–Thomson coefficient μ^0).

The calculation of variations of the diffusion coefficient D_{12} for mixtures of water vapor with nonpolar gases (H_2O–CO_2, H_2O–N_2, and H_2O–H_2) at $P = 1$ atm and $T = 79°C$ showed that at the quantum numbers $n \le 4$ and $J \le 10$ the maximum variation of the diffusion coefficient due to rotational-vibrational excitation of the water vapor molecule is insignificant; it equals roughly 3% for the considered gas mixtures and falls at the state (040).

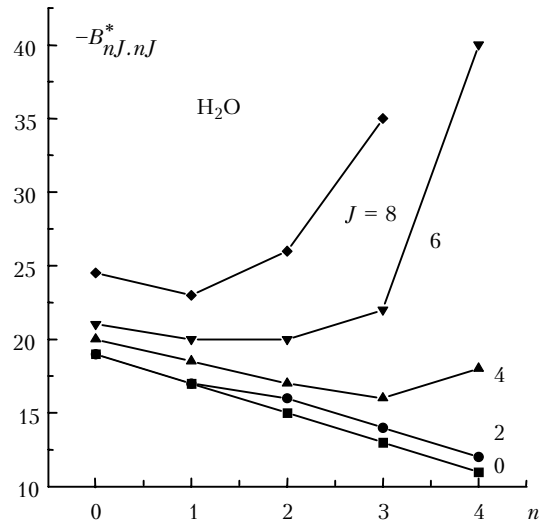

Fig. 3. Variations of reduced second virial coefficient B^* for water vapor ($T = 380$ K) in limiting case that all molecules are in the same rotational-vibrational state ($0\ v_2 \equiv n\ 0$) [J, $K_a = J$, $K_c = 0$].

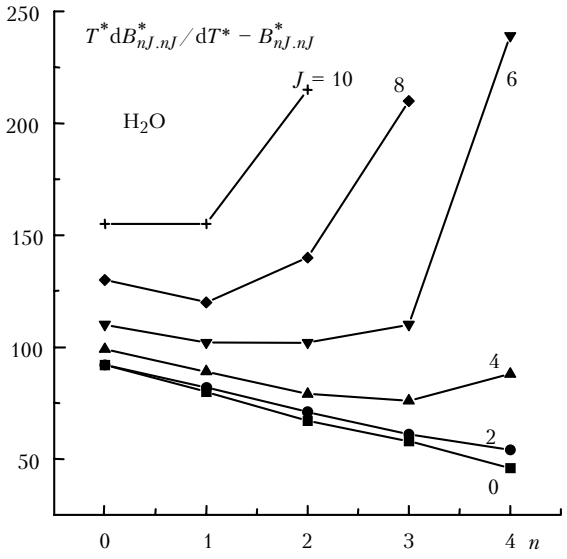

Fig. 4. Variations of difference $B_1^* - B^* = T^*\ dB^*/dT^* - B^*$ determining the Joule–Thomson coefficient μ^0 for water vapor ($T = 100°C$) in the limiting case when all molecules are in the same rotational-vibrational state.

Conclusions

The quantitative analysis of the problem has shown that variations of the dipole moment of the water vapor molecule due to excitation of large-amplitude modes and strong rotational-bending interaction lead to significant variations of some thermodynamic parameters of water vapor and the mixture of water vapor with other gases. Strong dependence of the coefficients determining the energy of a state, regardless of the fact that these are the virial

coefficients $B(T)$, $C(T)$ or the Van-der-Waals coefficient, has been demonstrated. In the considered processes, the electromagnetic energy initially deposited in the medium can initiate avalanche-type macroprocesses of removing the extra supersaturation in the atmosphere, which far exceed it by the released energy.

In the further research, it is interesting to study the specific radiative and kinetic mechanisms of excitation of water vapor molecules, first of all, to metastable rotational-vibrational levels with the participation of buffer atmospheric gases like CO_2, N_2, N_2O, O_3, and others.

Acknowledgments

The work was partially supported by the Russian Foundation for Basic Research, Grant No. 99–05–64885.

References

1. V.V. Zuev, A.A. Zemlyanov, Yu.D. Kopytin, and A.V. Kuzikovskii, *High-Power Laser Radiation in Atmospheric Aerosols* (D. Reidel Publ. Co., Dordrecht, 1985), 291 pp.
2. E.T. Protasevich, Yu.D. Kopytin, L.K. Chistyakova, and V.I. Shishkovskii, *Action of Laser and HF radiation on Air Medium* (Nauka, Novosibirsk, 1992), 190 pp.
3. S.F. Balandin and Yu.D. Kopytin, in: *Abstracts of Papers at VI Int. Symposium on Atmospheric and Ocean Optics*, Tomsk, Russia (1999), p. 75.
4. V.E. Zuev, Yu.D. Kopytin, E.T. Protasevich, and V.A. Khan, Dokl. Akad. Nauk SSSR, Ser. Fizika **294**, 453–458 (1986).
5. Yu.D. Kopytin and G.A. Mal'tseva, Izv. Vyssh. Uchebn. Zaved. SSSR, Ser. Fizika, No. 3, 95–101 (1978).
6. V.P. Grigoryev and E.T. Protasevich, *Der Kondensations-Koagulations Mechanismus Der Niederschlagsbildung* (Institute of Strength Physics at Tomsk Polytechnic University, Tomsk, 1994).
7. V.I. Starikov, Yu.D. Kopytin, and A.E. Protasevich, in: *Abstracts of Papers at VI Int. Symposium on Atmospheric and Ocean Optics*, Tomsk, Russia (1999), p. 74.
8. V.I. Starikov and Vl.G. Tyuterev, *Intramolecular Interactions and Theoretical Methods in Spectroscopy of Non-Rigid Molecules* (Institute of Atmospheric Optics SB RAS, Tomsk, 1997), 230 pp.
9. J.O. Hirshfelder, Ch. Curtiss, and R.B. Bird, *Molecular Theory of Gases and Liquids* (John Willey and Sons., INC., New York; Chapman and Hall, Lim., London, 1954).
10. V.I. Starikov and S.N. Mikhailenko, J. Mol. Structure **271**, 119–131 (1992).
11. J.T. Hougen, P.R. Bunker, and J.W.C. Johns, J. Mol. Spectrosc. **34**, 136 (1970).
12. V.I. Starikov, B.N. Machancheev, and Vl.G. Tyuterev, J. Phys. Letters **45**, L11 (1992).
13. A.R. Hoy, I.M. Mills, and G. Strey, Mol. Phys. **24**, 1265 (1972).
14. J.W. Cooley, Math. Comput. **15**, 363 (1961).
15. J.K.G. Watson, J. Chem. Phys. **46**, No. 5, 1935 (1967).
16. V.I. Starikov, S.A. Tashkun, and Vl.G. Tyuterev, J. Mol. Spectrosc. **151**, 130–147 (1992).
17. M. Mengel and P. Ensen, J. Mol. Spectrosc. **169**, 73–91 (1995).
18. I.G. Kaplan, *Introduction into Theory of Intermolecular Interactions* (Nauka, Moscow, 1982), 311 pp.